Materials & Design 264 (2026) 115796

Contents lists available at ScienceDirect

Materials & Design

journal homepage: www.elsevier.com/locate/matdes

A unified spatial Poisson's ratio design method (SPRDM) for 3D Poisson's ratio metamaterials based on a minimal chiral structure

Pierre Roberjot *, Rosalinde van den Bergh, Just L. Herder

Delft University of Technology, Department of Precision and Microsystems Engineering, Mekelweg 2, 2628CD Delft, the Netherlands

ARTICLE INFO

Keywords:
Metamaterials
Poisson'sratio
Rationaldesign
Auxetic
Meiotic
Anepirretic

ABSTRACT

Poisson's ratio metamaterials exhibit unconventional deformation behaviors enabled by architected internal geometries. While numerous planar auxetic and related designs have been reported, the systematic generation and classification of spatial Poisson's ratio metamaterials remains limited. In this work, we introduce the Spatial Poisson's Ratio Design Method (SPRDM), a unified geometric framework that extends a previously established planar design approach to three-dimensional architectures.

The SPRDM is built on two minimal kinematic bases, a planar and a spatial chiral structure and eight symmetry-based topological transformations that enable controlled manipulation of dimensionality and chirality. The method systematically generates 1.5D, 2D, 2.5D, and 3D metamaterial families, reproducing known auxetic, anepirretic, and meiotic architectures as well as enabling the design of previously unreported spatial and superchiral structures. A consistent classification scheme and naming protocol are introduced to organize the resulting design space, together with a unit-cell construction strategy supporting planar tessellations and three-dimensional honeycombs.

Representative examples demonstrate the versatility of the method, including spatial auxetic and anepirretic architectures with tunable deformation mechanisms. Volume strain is employed as a general metric to characterize compressibility beyond directional Poisson's ratios. The SPRDM provides a systematic foundation for the design of spatial Poisson's ratio metamaterials with broad relevance to architected materials research.

1. Introduction

Poisson's ratio metamaterials derive their unusual mechanical responses from architected internal geometries rather than intrinsic material properties [1]. By tailoring topology, these systems can exhibit auxetic (negative Poisson's ratio) [2,3], anepirretic (zero Poisson's ratio) [3,4], or meiotic (Positive Poisson's ratio usually greater than 0.5) [5–7] behavior, enabling applications ranging from energy absorption and vibration isolation to deployable systems [8], textiles [9–12] and soft robotics [13–17].

To date, the majority of Poisson's ratio metamaterials have been developed in planar or quasi-planar configurations. Numerous two-dimensional auxetic and anepirretic lattices have been proposed using rotating units, re-entrant geometries, chiral mechanisms, and modular linkages [15,18–20]. While these approaches have yielded a rich design space [21], their extension to fully three-dimensional architectures often relies on ad hoc extrusion, stacking, or intuition-driven generalization, limiting systematic exploration and classification.

Recent studies have demonstrated the potential of three-dimensional Poisson's ratio metamaterials with tunable and multi-functional responses, including double-negative auxetic architectures [22–24], modular energy-absorbing systems, and chiral lattices exhibiting coupled strain–twist behavior [7,25,26]. Despite these advances, a unifying design framework that connects planar and spatial architectures, rationalizes chirality across dimensions, and enables the controlled generation of both known and novel structures remains largely absent.

In prior work, we introduced a minimal planar chiral Poisson's ratio base structure and the associated Planar Poisson's Ratio Design Method (PPRDM), which systematically generates a wide range of planar auxetic, anepirretic, and meiotic metamaterials through a small set of symmetry-based transformations [27,28]. While this PPRDM captures most known planar topologies, certain spatial architectures particularly those involving intrinsic three-dimensional chirality or strain–twist coupling cannot be constructed from planar bases alone.

In this work, we extend this generative philosophy to the spatial

* Corresponding author.
E-mail address: p.roberjot@tudelft.nl (P. Roberjot).

https://doi.org/10.1016/j.matdes.2026.115796
Received 3 October 2025; Received in revised form 3 March 2026; Accepted 4 March 2026
Available online 6 March 2026

domain by introducing the Spatial Poisson's Ratio Design Method (SPRDM). The method is founded on two minimal kinematic bases: a planar base (Z_2) and its spatial counterpart (Z_3). From these bases, SPRDM employs eight topological transformations to systematically generate 1.5D, 2D, 2.5D, and 3D Poisson's ratio metamaterials while explicitly accounting for dimensionality, chirality, and tessellation capability.

Beyond structure generation, our SPRDM provides a unified classification scheme based on spatial dimensionality and chirality order, including the introduction of spatial superchirality. The framework enables the reconstruction of existing planar and spatial metamaterial families and reveals previously unreported architectures, including fully three-dimensional auxetic and anepirretic systems. Selected examples illustrate how the method supports the design of spatially tessellable unit cells, tubular and polyhedral architectures, and application-inspired groups such as anepirretic and deployable structures.

By framing Poisson's ratio metamaterials as outcomes of a limited set of topological operations rather than isolated geometries, the SPRDM offers a systematic pathway for the rational design, classification, and extension of architected materials across length scales.

2. Methods

This section introduces the Spatial Poisson's Ratio Design Method (SPRDM), a symmetry-based framework for generating planar and spatial Poisson's ratio metamaterials from minimal chiral base structures. The method defines dimensionality, chirality order, and a consistent naming protocol to classify architectures generated through topological transformations.

2.1. Z_2–Z_3: Minimal planar and spatial chiral base structures

This work builds on a minimal chiral Poisson's ratio base structure previously introduced for planar auxetic and meiotic metamaterials, denoted $\boldsymbol{Z_2}$ [1,2]. As shown in Fig. 1, Z_2 consists of three coplanar rigid beams ($[A'A] = a_1$, $[AB] = a_2$, $[BB'] = a_3$) connected by two revolute joints at points A and B. Its mechanical character is governed by the beam angles θ_1 and θ_2 (Fig. 1**.a**). The midpoint O of beam $[AB]$ defines the reference for strain evaluation, while the edge points $E_1 = A'$ and $E_2 = B'$ serve as connection interfaces between adjacent units. A continuous transition between auxetic and meiotic behavior occurs at the transition angle θ_T, to a right-triangle configuration at O, where $\theta_1 = \theta_2 = \theta_T$, where:

$$cos(\theta_T) = \frac{a_2}{2a_1} \tag{1}$$

Starting from Z_2, the **Planar Poisson's Ratio Design Method (PPRDM)** generates planar Poisson's ratio metamaterials through two symmetry-based transformations: achiralisation (ACR), which mirrors a chiral unit about an achiralisation axis, and copy-rotation (CR), which replicates a unit N times about a rotation center with sector angle $\varphi_N = 360^\circ/N$. Together, these operations enable the systematic reconstruction of most known planar auxetic, anepirretic, and meiotic lattices (Fig. 1**,a-d**). The description of the twelve regular planar bases is given in **Supplementary information SI.1**.

To extend this framework into three dimensions, we introduce $\boldsymbol{Z_3}$, a spatial generalization of Z_2 that serves as the minimal spatial chiral base for the **Spatial Poisson's Ratio Design Method (SPRDM)**. As shown in Fig. 1**.e** Z_3 preserves the topology of Z_2 but rotates one outer beam (AA' or BB') out of the plane by an angle ω, tilting the corresponding revolute joint accordingly. Z_3 is a spatial chiral structure composed of three rigid beams and two non-coplanar joints. When $\omega = 0^\circ$, Z_3 reduces exactly to the planar Z_2 topology.

The Z_3 unit can be tessellated along a single direction by rigidly connecting its edge points $A' = E_1$ and $B' = E_2$, forming a prismatic or tubular envelope. Axial strain is evaluated analogously to Z_2 from point O; however, due to the non-coplanar joint orientations, Z_3 exhibits an intrinsic strain–twist coupling. As a result, Poisson's ratio alone is insufficient to fully characterize its mechanical response, motivating the strain–twist formalism [25–29].

Together, Z_2 and Z_3 provide a unified minimal foundation for planar and spatial Poisson's ratio metamaterials.

2.2. Spatial Poisson's ratio design Method (SPRDM)

The **Spatial Poisson's Ratio Design Method (SPRDM)** extends the PPRDM to enable the systematic generation and classification of spatial Poisson's ratio metamaterials. The SPRDM unifies dimensionality, chirality, and symmetry-based construction within a single generative framework.

2.2.1. Dimensional classification

The Poisson's ratio metamaterials are classified according to the spatial arrangement of their connection edges E_n, which determines their tessellation capability:

- **1.5D structures** possess collinear edges and tessellate naturally along a line. Both Z_2 and Z_3 belong to this class.
- **2D and 2.5D structures** have coplanar edges. Fully planar (2D) structures tessellate only in a plane, whereas 2.5D structures retain coplanar edges but include spatial internal geometry, allowing both planar and spatial tessellation.
- **3D structures** exhibit edges distributed in three dimensions, typically inscribed in spherical or tubular geometries, enabling full three-dimensional tessellation.

This classification decouples geometric embedding from internal kinematics and allows planar and spatial architectures to be treated within a unified framework.

2.2.2. Chirality and superchiral order

Beyond dimensionality, chirality plays a central role in spatial

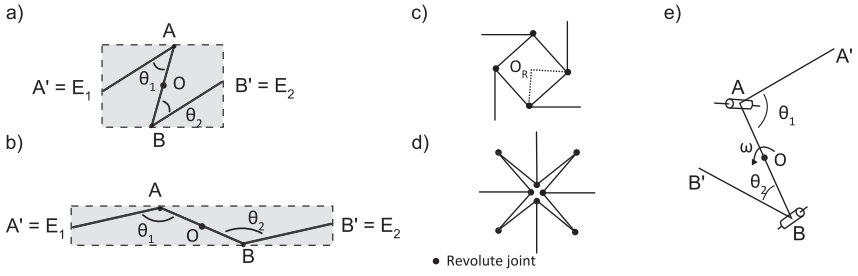

Fig. 1. Representation of the base structure Z_2 in its (a) auxetic and (b) meiotic shape with their points of interest. The PPRDM can be applied to Z_2 with the two planar topological transformations ACR and CR yielding to the examples of (c) the chiral (χ_1) Hc4 and (d) the achiral (χ_0) 4CCs. The spatial base Z_3 (e) is built from Z_2 by rotating the revolute joint relative to each other about the center line of the middle beam.

Poisson's ratio metamaterials. We define a **chirality order** χ, given by:

$$\chi = d - 1 - a \quad (2)$$

where d is the minimum number of spatial dimensions required to define the structure and a the number of applied chirality reduction transformations (Table 1). Accordingly:

- χ_0 denotes achiral structures,
- χ_1 denotes chiral structures (e.g., the planar structure Z_2, the spatial structure $M3r4$),
- χ_2 denotes spatially superchiral structures (e.g., Z_3).

A superchiral structure requires multiple independent achiralisation operations to become fully achiral, with each achiralisation a reducing χ by one. Starting from Z_2, the SPRDM generates structures with $\chi \in \{0, 1\}$, whereas starting from Z_3 enables access to $\chi \in \{0, 1, 2\}$. This distinction is essential for spatial architectures, where some transformations preserve chirality order while others reduce it.

2.2.3. SPRDM workflow

The Spatial Poisson's Ratio Design Method (SPRDM) follows a structured three-stage workflow:

- ***Base selection***
  The design process starts from either the planar chiral base structure Z_2 or its spatial counterpart Z_3, depending on the targeted dimensionality and chirality class of the metamaterial.
- ***Chirality management***
  Achiralisation and chirality-preserving operations are applied to control the chirality order χ while maintaining kinematic compatibility of the underlying linkage architecture.
- ***Spatial assembly***
  Copy-rotation–based transformations are then employed to generate linear (1.5D), planar (2D/2.5D), or fully spatial (3D) tessellations.

  The SPRDM is implemented through eight symmetry-based topological transformations (Table 1), comprising two planar operations inherited from the Planar Poisson's Ratio Design Method (PPRDM) and six spatial extensions. In the main manuscript, these transformations are introduced at a functional level within the overall workflow (Fig. 2) and illustrated through representative existing and newly generated structures, emphasizing their design logic and generative capabilities. The **Supplementary Information SI.3.** serves as a technical reference for the method: it contains the complete geometric definitions, formal construction rules, higher-order variants, and extended naming conventions for each transformation. This separation allows the main text to remain focused on the conceptual architecture of SPRDM, while preserving a full implementation-level description for readers interested in reproducing or extending the framework.

2.3. Naming convention

To ensure clarity and traceability across the large design space generated by the SPRDM, a compact and modular naming convention is adopted. Structure names encode the originating base or family, the applied transformations and their order, the design type (chiral, achiral, classical, or reciprocal), and the resulting dimensionality.

Rather than serving as an exhaustive enumeration, the naming convention functions as a concise design shorthand, enabling unambiguous reference to complex spatial architectures while keeping the main text readable. Representative examples are provided in Fig. 3, and the convention is used consistently throughout the Results section. The details of the naming convention are provided in the **Supplementary information SI.2.**

2.4. Unit cell, tessellation and honeycombs

The unit cells generated by SPRDM follow a systematic Voronoi-based construction that links each transformation to a unique tessellation geometry. Planar structures produce polygonal primitive cells that tile the plane through regular or semi-regular tessellations, while spatial transformations generate polyhedral unit cells that assemble into three-dimensional honeycombs. This framework ensures geometric compatibility between local linkage kinematics and global tiling behavior, allowing SPRDM designs to be extended from single mechanisms to space-filling metamaterials. The complete geometric construction rules for unit cells, tessellations, and honeycombs are provided in **Supplementary Information SI.4**, where the Voronoi protocol and spatial cell taxonomy are detailed.

2.5. Scope of the method

Using this workflow, the SPRDM generates **30 regular Poisson's ratio metamaterial families** (13 planar and 17 spatial), which can be further extended into irregular and hybrid architectures. The method emphasizes **topological generation rather than geometric optimization**, providing a structured design space for auxetic, meiotic, anepirretic, and strain–twist metamaterials.

Detailed descriptions of the eight transformations, along with representative applications and mechanical implications, are presented in **Section 3**.

3. Results: Application of the SPRDM to planar and spatial metamaterials

This section demonstrates how the Spatial Poisson's Ratio Design Method (SPRDM) generates planar and spatial Poisson's ratio metamaterials from minimal base structures. Rather than exhaustively cataloguing all possible configurations, we focus on (i) the role of the eight topological transformations, (ii) representative design pathways leading to known and novel architectures, and (iii) selected classes of application-relevant metamaterials. Detailed derivations, irregular

Table 1
Overview of the eight topological transformations constituting the Spatial Poisson's Ratio Design Method (SPRDM), indicating their dimensional role, effect on chirality order χ, and primary design function. Detailed geometric definitions and representative structures generated by each transformation are presented in the Results section.

Transformation	Type	Function in SPRDM	Dimensional effect	Chirality effect
ACR (Achiralisation)	Planar / Spatial	Mirrors a chiral structure to form an achiral topology	Preserves dimension	$\chi\downarrow$ (reduces chirality order)
CR (Copy-rotation)	Planar	Generates planar chiral or achiral lattices via rotational symmetry	1.5D → 2D	χ preserved
aCR (Axis copy-rotation)	Spatial	Extends achiralisation into 3D by rotation about an axis	1.5D → 2.5D / 3D	$\chi\downarrow$
tCR (Tube copy-rotation)	Spatial	Forms tubular and prismatic spatial architectures	1.5D / 2D → 3D	χ preserved
LCR (Line copy-rotation)	Spatial	Generates chain-like and strain–twist structures	1.5D → 1.5D / 3D	χ preserved
pCR (Pyramidal copy-rotation)	Spatial	Assembles polyhedral unit cells (Platonic/Archimedean)	2D / 2.5D → 3D	$\chi\downarrow$
sCR (Surface copy-rotation)	Spatial	Intersects planar chiral lattices to form 3D chiral cells	2D → 3D	χ preserved
PrCR (Prism copy-rotation)	Spatial	Generates auxetic prism-based architectures	2D → 3D	$\chi\downarrow$

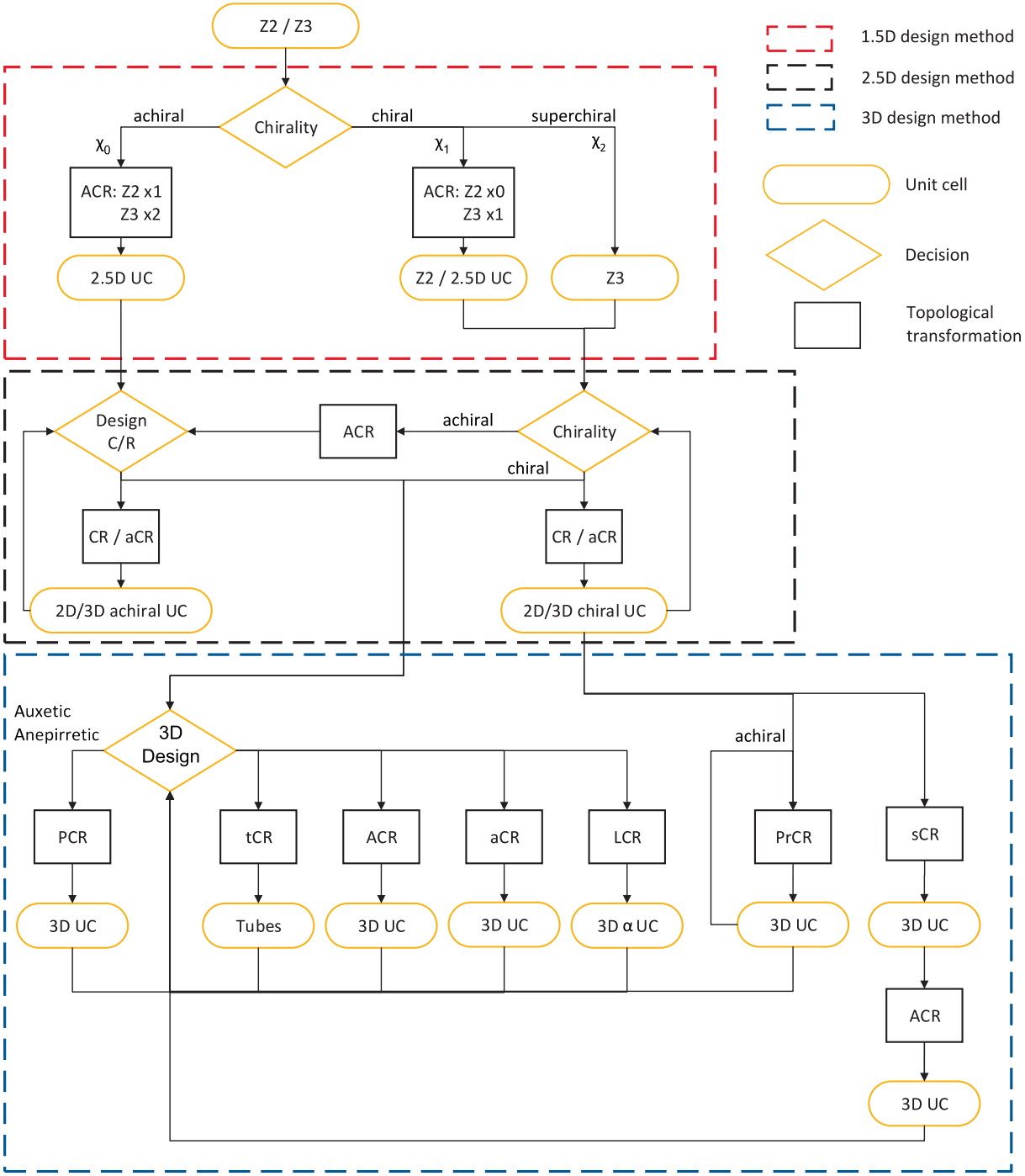

Fig. 2. Schematic overview of the Spatial Poisson's Ratio Design Method (SPRDM). The workflow starts from either the planar base structure Z_2 or the spatial base structure Z_3, followed by chirality control and dimensional expansion through symmetry-based topological transformations. The method enables the systematic generation of 1.5D, 2D, 2.5D, and 3D Poisson's ratio metamaterials within a unified design framework.

cases, and extended taxonomies are provided in the Supplementary Information.

3.1. Topological transformations: Functional overview and representative outcomes

The SPRDM relies on eight symmetry-based topological transformations that act on the base structures Z_2 and Z_3, as shown in Fig. 2. In this section, these transformations are introduced through their functional effects and representative structures, while their formal definitions and construction rules are summarized in Table 1 and detailed in the Methods and **Supplementary Information SI.3**.

The transformations can be grouped into three functional categories:

1. Chirality-control transformations
2. Achiralisation (ACR) and axis copy-rotation (aCR) control the chirality order χ by combining mirror images or distributing copies around an axis.
3. Dimensional expansion transformations
4. Copy-rotation (CR), tube copy-rotation (tCR), pyramidal copy-rotation (pCR), surface copy-rotation (sCR) [30,31], and prism

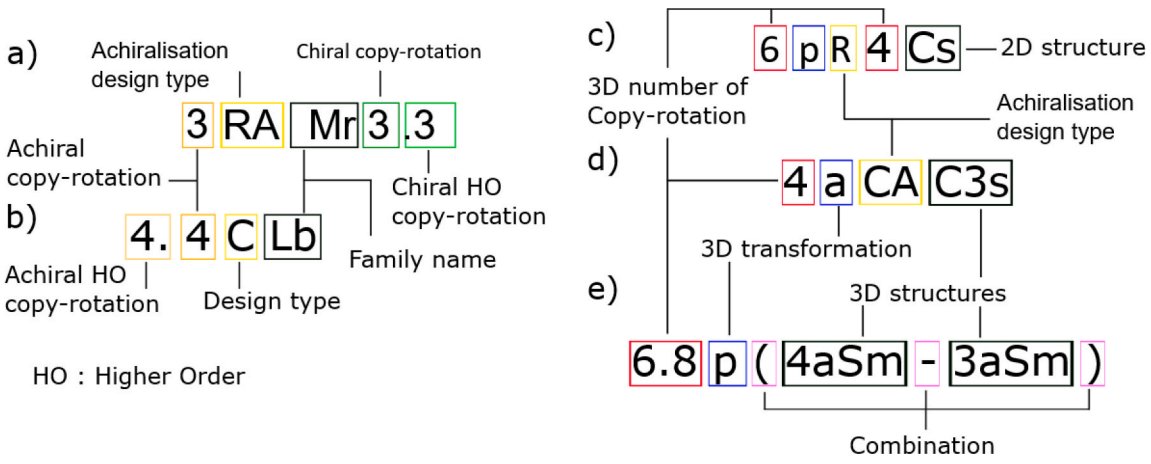

Fig. 3. Examples illustrating the SPRDM naming convention. Structure names encode the originating base or family, applied topological transformations, chirality state, and dimensional class, enabling compact and unambiguous reference to complex planar and spatial Poisson's ratio metamaterials. Examples include (a) a planar auxetic structure 3RAMr3.3, (b) a planar meiotic structure 4.4CLb, spatial structures derived from (c) Z_2 (6pR4Cs) and (d) Z_3 (4aCAC3s), and (e) a combined hierarchical structure 6.8p(4aSm −3aSm).

copy-rotation (PrCR) [32,33] enable the transition from 1.5D to 2D, 2.5D, and fully 3D architectures.

5. Connectivity-modifying transformations Line copy-rotation (LCR) introduces chained and junction-like geometries that can subsequently be expanded spatially.

Together, these transformations allow the systematic generation of regular planar and spatial Poisson's ratio metamaterials families, as well as their extension to higher-order and hybrid configurations. The eight transformations are illustrated here through representative outcomes; their formal definitions and irregular extensions are detailed in **Supplementary Information SI.3**.

3.2. Design examples: From base structures to known and novel architectures

3.2.1. Example I – Reconstruction of known planar and spatial auxetic lattices

Starting from the planar base Z_2 in its auxetic configuration Z_A, the application of ACR and CR reproduces classical planar auxetic families such as Connected Stars (*Cs*), Puzzle Tiles (*Pt*), Rotating Triangles (*Rt*), Honeycomb (*Hc*), and Missing-rib (*Mr*). These families encompass many widely studied auxetic lattices reported in the literature.

Extending these planar families spatially, tube copy-rotation (tCR) applied to planar auxetic bases generates tubular auxetic structures such as *Nt2CCs* [16,34] or 2*RAHc*4 [7], while pyramidal copy-rotation (pCR) enables the construction of cubic and prismatic 3D auxetic lattices (e.g., 6*pC*4*Cs*) [8,35,36]. The line copy-rotation (LCR) enables the construction of fiber-like or mesh-like 3D topologies (e.g., 4*a*2*LCs*). These results demonstrate that SPRDM naturally recovers a large class of existing auxetic metamaterials within a unified topological framework. The

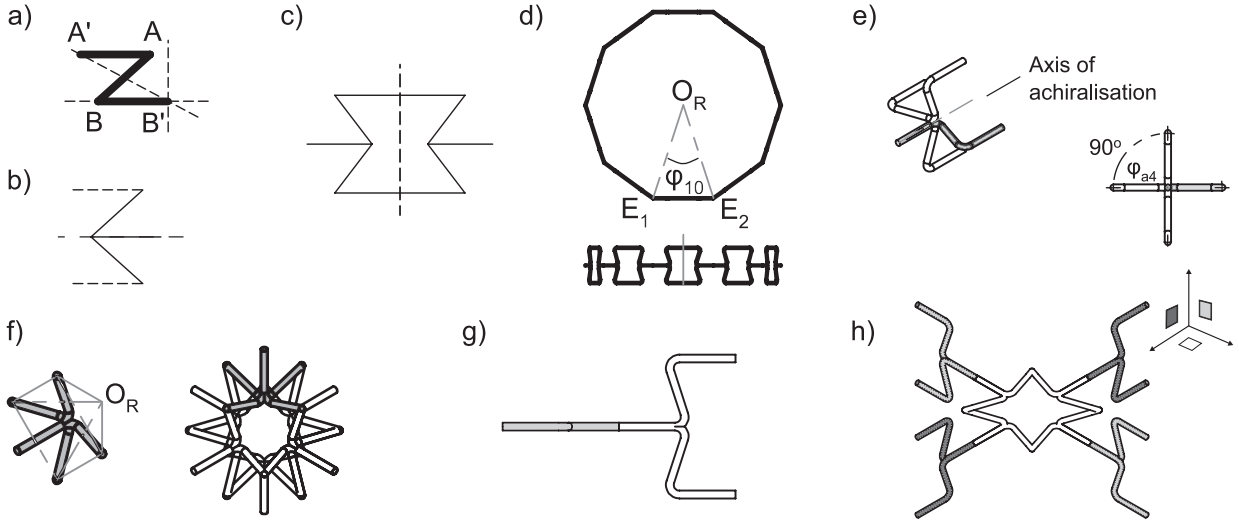

Fig. 4. Illustration of the Spatial Poisson's Ratio Design Method (SPRDM) applied to (a) the planar auxetic base Z_A. (b) Selection of the BB′ axis for achiralisation (ACR), yielding the auxetic base Connected Stars (Cs). (c) Planar copy-rotation (CR) of Cs to form the structures 2CCs. These planar architectures can serve as inputs for spatial transformations, illustrated by (e) the tube copy-rotation (tCR) of 2CCs generating the tubular structure Nt2CCs. In addition, spatial auxetic topologies can be obtained directly from Z_A via axis copy-rotation (aCR), illustrated by (f) the structure 4Cs, which can be further transformed using (g) pyramidal copy-rotation (pCR) to form the fully spatial architecture 6p4Cs. The Cs base can be used as an input in the (g) line copy rotation (LCR) to form the structure 2LCs which can be transformed for instance with aCR into (h) 4a2LCs.

illustration of the SPRDM applied to the Connected stars (*Cs*) is presented in Fig. 4.

3.2.2. Example II – Novel spatial chiral and strain–twist metamaterials from Z_3

Using the spatial base Z_3 introduces an additional degree of freedom through non-coplanar joints, leading to spatially chiral (χ_2) structures. Line copy-rotation (LCR) does not reduce the order of chirality but when applied to Z_3 limits to structures like $2.2LZ_3$. Axis copy-rotation (aCR) of Z_3 generates novel 3D chiral families such as *M3r*, *H3c*, and *C3g*, which have no direct planar analogue. These transformations and structures are illustrated in Fig. 5.

These structures exhibit coupled axial strain and twist, a behavior not captured by classical Poisson's ratio alone. For instance, tubular structures derived from Z_3 through tCR display screw-like deformation under axial loading, combining auxetic or meiotic behavior with controlled rotation. Such architectures extend the design space toward strain–twist and micropolar metamaterials and provide a systematic route to geometries previously reported only as isolated designs. The mechanical behavior of micropolar metamaterials has been described using Cosserat, couple stress and micropolar theories [25,37–39].

3.2.3. Example III – Fully achiral 3D architectures and space-filling lattices

By applying achiralisation twice to Z_3, the SPRDM generates fully achiral (χ_0) spatial base families, including *C3s*, *L3b*, *P3t*, and *R3o*. The spatial base Z_3 can also be achiralised (ACR) one time in six main χ_1 structures namely *H2c*, *M2r*, *C2g*, *HcA*, *MrA* and *CgA*. These bases can be further expanded using aCR, tCR, and pCR to produce space-filling or partially space-filling lattices. The structures formed by the bases *C3s* and *MrA* are presented in Fig. 6.

Notably, several of these structures form cubic, prismatic, or Archimedean unit cells compatible with known space-filling honeycombs. This capability enables the rational design of bulk 3D metamaterials with controlled isotropy or directional response, highlighting the SPRDM as a generative rather than case-specific approach. The space filling honeycombs are presented and illustrated in **supplementary information SI.4**.

3.3. Remarkable groups of application-inspired metamaterials

Beyond individual examples, the SPRDM naturally gives rise to several **remarkable families** of Poisson's ratio metamaterials with distinct mechanical significance. Four such families are highlighted below.

3.3.1. Anepirretic metamaterials (zero Poisson's ratio)

Anepirretic metamaterials, characterized by a zero Poisson's ratio, emerge naturally within the SPRDM through reciprocal transformations of achiral bases. Planar square anepirretic structures (e.g., 4*RCs*) and cubic anepirretic lattices (e.g., 6*pR4Cs*) are obtained without additional constraints (Fig. 7) [3,4,40].

Importantly, the SPRDM distinguishes between **partial anepirretic** structures (zero Poisson's ratio in selected directions) and **full anepirretic** structures (zero Poisson's ratio in all orthogonal directions). This distinction enables the systematic design of lattices with decoupled deformation modes, which are relevant for precision mechanisms, deployable systems, and vibration isolation.

3.3.2. Hoberman-type deployable mechanisms

The SPRDM reproduces and generalizes Hoberman-type deployable mechanisms by combining axis copy-rotation (aCR) with pyramidal copy-rotation (pCR) applied to scissor-like bases, illustrated in Fig. 8. These structures preserve a single degree of freedom while exhibiting auxetic deployment, including spherical and polyhedral Hoberman geometries. Their compatibility with space-filling or modular assemblies makes them attractive for deployable and robotic applications [41–43].

3.3.3. Helical auxetic Yarns (HAYs)

Helical Auxetic Yarns (HAYs) are auxetic structures composed of *N* twisted fibers [44–46]. HAYs are interpreted within the SPRDM as 1.5D chiral architectures derived from a combination of Z_2 and Z_3-based structures (Fig. 9). The framework unifies previously reported 2-ply and

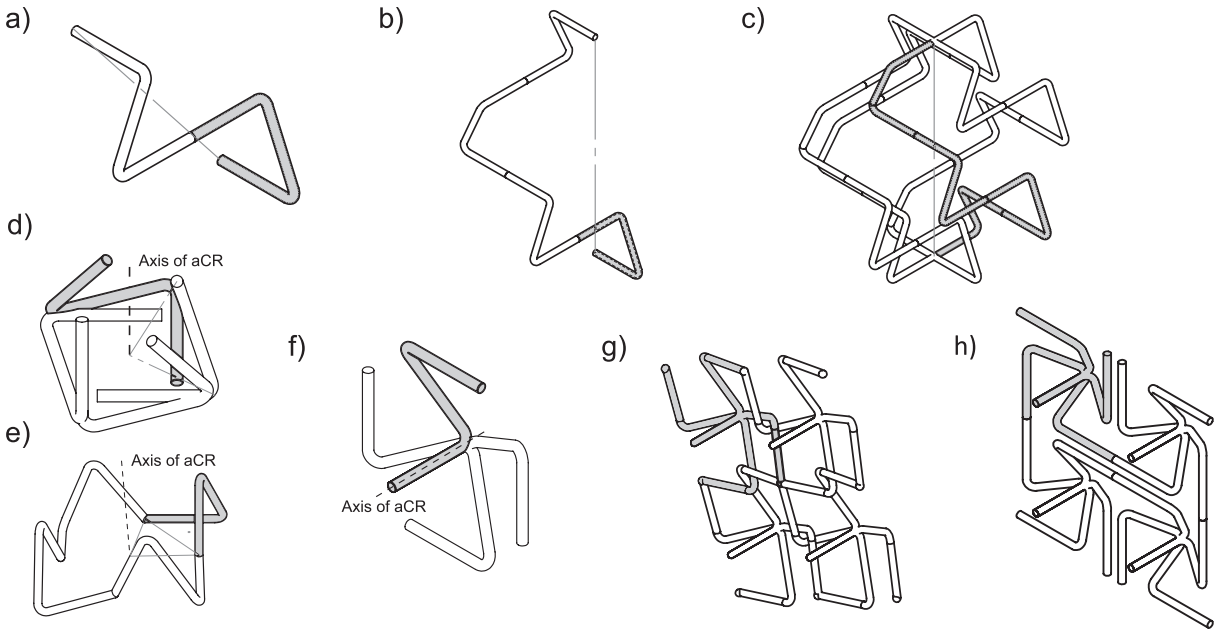

Fig. 5. Application of the SPRDM to the spatial base Z_3, illustrating superchirality management and spatial family generation. (a) Line copy-rotation (LCR) applied to Z_3 yielding the χ_2 superchiral structure $2LZ_3$, and (b) repeated LCR producing $2.2LZ_3$. (c) Axis copy-rotation (aCR) applied to $2.2LZ_3$ reduces the superchirality order, generating the χ_1 structure 4a2.2LZ_3. Direct application of aCR to Z_3 enables the systematic generation of χ_1 spatial families, illustrated by (d–f) the structures H3c4, C3g4, and M3r4. These χ_1 structures can be further processed within the SPRDM workflow (Fig. 2), for example by (g) higher-order axis copy-rotation yielding M3r4.4, or by (h) achiralisation followed by copy-rotation to form the achiral structure 2CAM3r4.

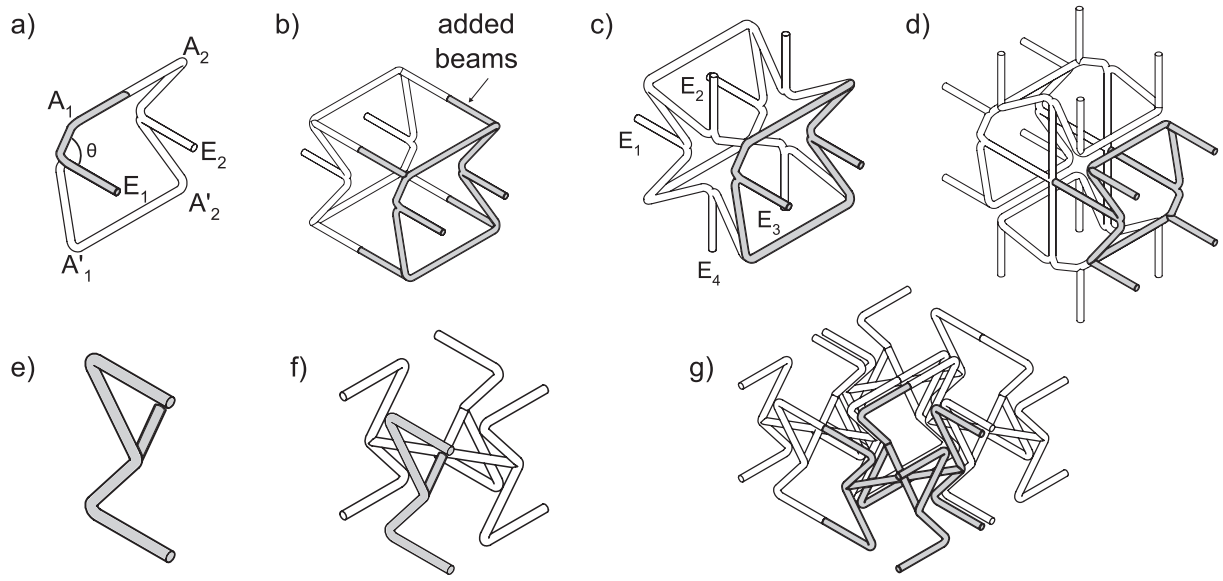

Fig. 6. Application of the SPRDM to achiral and chiral spatial bases derived from Z_3. (a) Fully achiral (χ_0) spatial base C3s obtained through double achiralisation of Z_3. (b,c) Classical axis copy-rotation (aCR) of C3s yielding the structures 2aCC3s and 4aCC3s, and (d) the corresponding reciprocal design 4aRC3s. (e) Generation of the χ_1 spatial base MrA through single achiralisation of Z_3. (f) Axis copy-rotation of MrA producing the chiral structure MrA4, which can be further (g) achiralised and copy-rotated to form the achiral structure 2CAMrA4 [55].

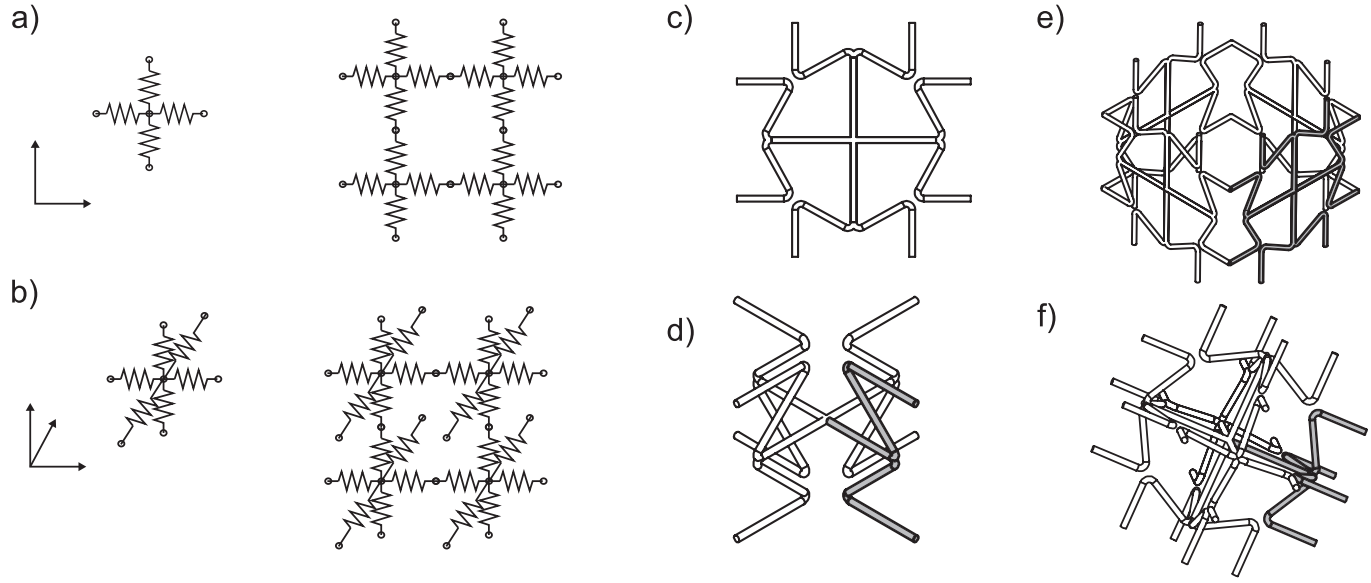

Fig. 7. Concept of anepirreticity illustrated through decoupled deformation along orthogonal directions: (a) planar (2D) anepirretic response and (b) spatial (3D) anepirretic response, where deformation in one principal direction does not induce strain in the others. Anepirretic metamaterials are generated from a topological decoupling point, illustrated by (c) the planar reciprocal structure 4RCs obtained via copy-rotation (CR), (d) the 2.5D structure 4aRCs obtained via axis copy-rotation (aCR), (e) the tubular anepirretic structure 4t4RCs generated through tube copy-rotation (tCR), and (f) the fully spatial anepirretic structure 6pR4Cs obtained via pyramidal copy-rotation (pCR), which decouples deformation along all three spatial directions.

N-ply HAYs and clarifies the role of chirality, twist, and auxetic expansion within a single topological description. This perspective enables systematic variation of yarn geometry, ply number, and deformation response.

3.3.4. *Hierarchical metamaterials*

Hierarchical Poisson's ratio metamaterials are obtained by nesting the SPRDM-generated unit cells across multiple length scales [47–49]. Both self-similar (fractal) and non-self-similar hierarchical architectures can be constructed, including mandala-like planar assemblies and spatially nested shells generated through pCR transformation. Such hierarchies enable enhanced tunability, energy absorption [50], and multifunctional behavior. Some topologies of hierarchical PR metamaterials with their naming convention are detailed in **Supplementary Information SI.5**.

3.4. *Limitations of Poisson's ratio and extension to strain–twist and volume strain*

Not all architectures generated by the SPRDM can be fully characterized by Poisson's ratio. By definition, Poisson's ratio relates orthogonal normal strains and therefore requires a square or cubic reference

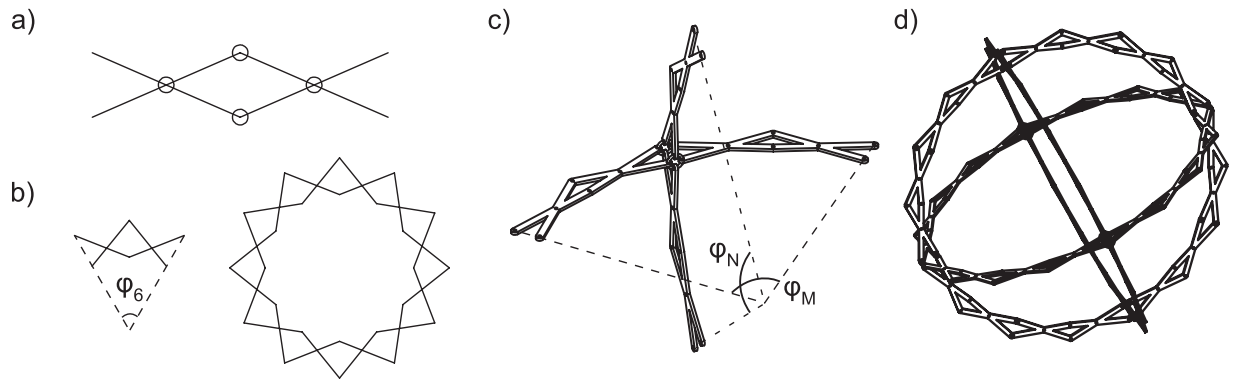

Fig. 8. Topological design of Hoberman-type deployable metamaterials within the SPRDM framework. (a) Meiotic scissor mechanism (Sm) serving as the planar base unit. (b) Planar Hoberman-type mechanisms obtained by copy-rotation (CR) of Sm. Spatial Hoberman mechanisms are generated through sequential spatial transformations, illustrated by (c) axis copy-rotation (aCR) of Sm into 4aSm followed by (d) pyramidal copy-rotation (pCR), yielding closed three-dimensional Hoberman-type architectures such as the deployable sphere 6p4aSm.

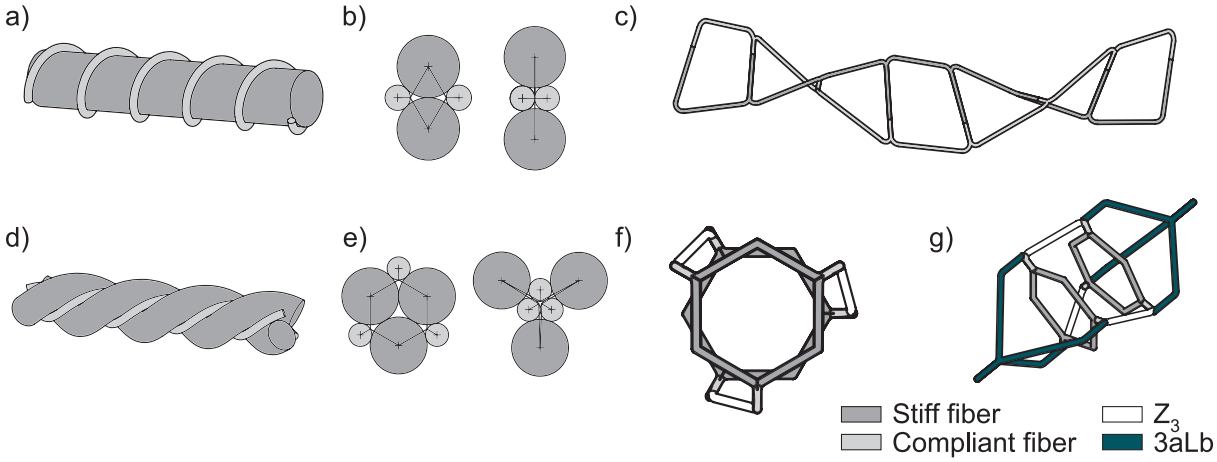

Fig. 9. Topological design of Helical Auxetic Yarns using the spatial base Z_3. (a) Schematic of a 2-ply HAYs and (b) its construction from paired Z_3 *s* topologies. N-ply HAYs are composed of N fibers whose cross sections correspond to planar auxetic structures, illustrated by (c) a 4-ply HAYs with cross-section topology 2CCs and (d) a 6-ply HAYs with cross-section topology 3CCs. In all cases, adjacent cross sections are connected by N/2 spatial Z_3 elements, defining the helical and auxetic response. The complete topology of an N-ply HAYs is fully determined by its two terminal edges and can be encoded using the SPRDM naming convention, e.g. (3aLb–3(CCs–Z_3)–3aLb) for a representative configuration.

frame. Many planar and spatial structures produced by the SPRDM lack a natural orthogonal basis or exhibit intrinsic rotational kinematics. In such cases, Poisson's ratio alone is insufficient to describe the mechanical response.

For planar Poisson's ratio metamaterials, surface strain was previously introduced as a direction-independent descriptor. In the spatial case, we extend this approach by introducing the **volume strain**

$$\varepsilon_V = \frac{V_F - V_I}{V_I} \tag{3}$$

which measures the global volumetric deformation of a unit cell. Volume strain is independent of coordinate orientation and is directly related to the bulk modulus and compressibility, providing a unified metric for comparing planar and spatial Poisson's ratio metamaterials.

3.4.1. Chiral and strain–twist metamaterials

The SPRDM naturally generates families of chiral metamaterials that exhibit a coupled strain–twist response. Typical examples are tubular structures of the form NtZ_A and NtZ_M, in which axial loading induces a rotation of the structure. By selecting the topology of the base *Z* structure, twist can be combined with auxetic, meiotic, or anepirretic behavior.

Such responses cannot be described by classical elasticity and require an extended framework such as micropolar (Cosserat) elasticity or Willis coupling, where rotations and couple stresses are included [37,51]. This places SPRDM-generated structures within the broader class of architected chiral media and significantly expands the accessible design space beyond Poisson's-ratio-based metamaterials. Additional hierarchical constructions and naming cases are presented in **Supplementary Information SI.5**.

3.4.2. Volume strain, compressibility, and negative compressibility

While Poisson's ratio is well defined for square and cubic unit cells, many architectures generated by the SPRDM lack a natural orthogonal reference frame. To address this limitation, volume strain (ε_V) is introduced as a direction-independent metric to characterize global deformation. As it is directly related to the bulk modulus (K_V) and compressibility (β_V), volume strain provides complementary mechanical insight beyond directional Poisson's ratios.

$$K_V = -\frac{\sigma}{\varepsilon_V}, \beta_V = \frac{1}{K_V} \tag{4}$$

Analysis of representative SPRDM-generated structures reveals three characteristic behaviors: (i) fully auxetic architectures exhibit a positive

bulk modulus and positive compressibility [52,53]; (ii) meiotic and partial auxetic architectures may display regions of negative linear or volumetric compressibility [5,54]; and (iii) anepirretic architectures maintain bounded volume strain over their deformation range.

Fig. 10 illustrates the evolution of volume strain for representative full and partial auxetic, anepirretic, and meiotic structures. In particular, meiotic and partial anepirretic architectures can exhibit negative compressibility over specific deformation regimes, a feature of interest for applications such as highly sensitive mechanical sensing. Fully auxetic architectures, by contrast, do not exhibit negative compressibility within the kinematically admissible range. Analytical derivations and parametric plots are provided in **Supplementary information SI.6.**

3.4.3. *Partial behaviors and programmable compressibility*

Structures such as tubular *Nt2CCs* and axis-rotated *4aRCs* display **partial behaviors**, where auxetic, anepirretic, and meiotic responses coexist depending on loading direction. In particular, the structure 4aRCs illustrates that a single topology can successively exhibit full anepirretic behavior, auxetic response, and negative compressibility depending only on its initial geometry and applied strain. This highlights the possibility of designing **programmable compressibility metamaterials** using the SPRDM.

Finally, the region defined by $\varepsilon_\theta < 0$ and $\varepsilon_V > 0$ is not attainable, as it would correspond to a material expanding in all directions under compression, implying a negative Young's modulus. This establishes a fundamental energetic limit for Poisson's ratio metamaterials.

4. Discussion

This work introduces the Spatial Poisson's Ratio Design Method (SPRDM) as a unified, geometry-driven framework for the systematic generation of planar and spatial Poisson's ratio metamaterials. Built upon the minimal bases Z_2 and Z_3 and a limited set of eight topological transformations, SPRDM provides a constructive pathway to generate auxetic, anepirretic, meiotic, and chiral metamaterial architectures across 1.5D, 2D, 2.5D, and 3D configurations.

A central contribution of the SPRDM lies in its generative character. Rather than optimizing a specific geometry or targeting a single mechanical metric, the method organizes a large design space through symmetry, connectivity, and kinematic principles. The results section therefore focused on a restricted number of illustrative transformations and examples, demonstrating how existing architectures reported in the literature can be recovered, while also revealing previously unexplored spatial families. Some extensions of the SPRDM with irregular cases, higher-order transformations and specifications of the naming protocol are detailed in **supplementary information SI.7**.

The dimensional and chirality-based classification introduced here clarifies long-standing ambiguities between planar, quasi-planar, and spatial Poisson's ratio metamaterials. In particular, the introduction of the superchirality order χ provides a compact way to distinguish planar chiral, spatial chiral, and fully achiral architectures, and to track how chirality evolves under topological transformations. This distinction becomes essential when extending planar design principles into three-dimensional space, where multiple independent achiralisation steps may be required.

Within this framework, the SPRDM enables the systematic design of full and partial auxetic and anepirretic structures, including spatial architectures that decouple deformation modes. The anepirretic families highlighted in the Results section illustrate how symmetry-controlled connectivity can suppress transverse strain in selected directions, extending classical planar anepirretic concepts into 3D lattices. These examples demonstrate that anepirreticity is not a marginal or accidental property, but can be intentionally encoded through topology.

At the same time, the SPRDM naturally generates chiral architectures for which the Poisson's ratio alone is insufficient to describe the mechanical response. Structures derived from Z_3 and certain spatial copy-rotation transformations exhibit coupled strain–twist behavior. Rather than treating these cases as exceptions, the SPRDM places them within the same generative framework. A generalized description based on volume strain and micropolar or Cosserat-type elasticity is therefore more appropriate for such architectures. Detailed formulations and parametric analyses of strain–twist coupling and volume strain responses are provided in the Supplementary Information, allowing the main manuscript to remain focused on the design methodology.

The method deliberately emphasizes regular topologies, which serve as reference architectures. However, the SPRDM also makes clear that irregularities—introduced through geometric tuning of base parameters, non-integer transformation orders, or heterogeneous tessellations—constitute a powerful secondary design layer. These irregular variants enable graded responses, directional effects, and localized functionalities, suggesting strong potential for application-driven refinement.

Several limitations should be acknowledged. First, the SPRDM is a topological and kinematic framework: it does not by itself predict

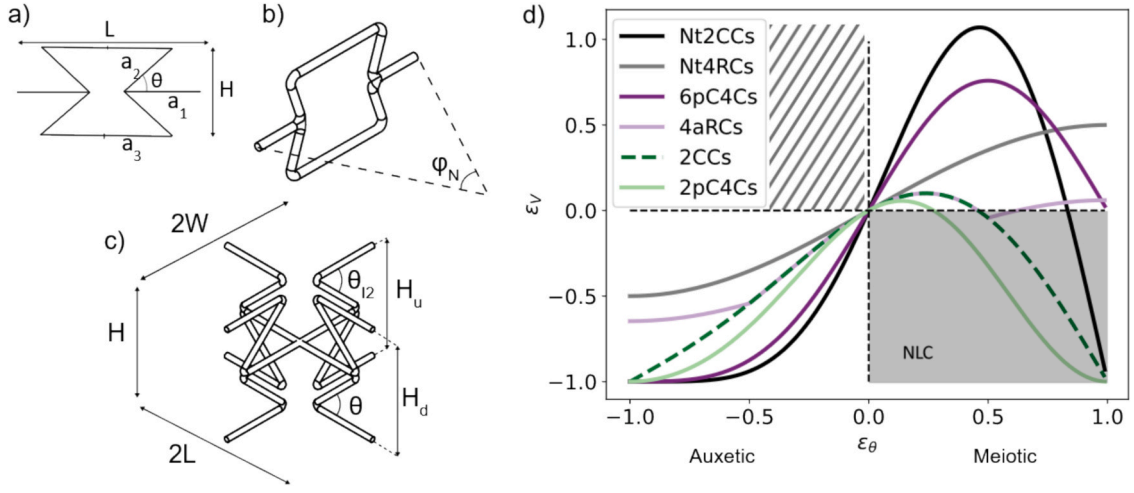

Fig. 10. Evaluation of volume strain for representative Poisson's ratio metamaterials. (a) Planar auxetic structure 2CCs, (b) tubular structure Nt2CCs obtained via tube copy-rotation, and (c) partial anepirretic structure 4aRCs obtained via axis copy-rotation. (d) Evolution of the volume strain ε_V as a function of deformation for auxetic, anepirretic, and meiotic architectures. Auxetic structures exhibit a strictly negative volume strain under compression, while meiotic structures may display regions of negative Linear compressibility (NLC). The partial anepirretic structure 4aRCs exhibits both positive and negative compressibility regimes depending on the applied strain.

stiffness, strength, stability, or failure, which depend on material choice, joint realization, and finite deformation effects. Second, although a wide range of known Poisson's ratio metamaterials can be generated within the SPRDM, a formal proof of completeness is beyond the scope of this work. Third, practical fabrication of spatial architectures, particularly those relying on ideal revolute or universal joints, remains challenging and may require approximation through compliant mechanisms, origami-inspired embodiments, or additive manufacturing strategies.

Overall, the SPRDM provides a unifying language and workflow for the design of planar and spatial Poisson's ratio metamaterials. By decoupling topological generation from mechanical optimization, the method establishes a foundation upon which simulation, experimental validation, and application-specific refinement can be systematically built. Future work will focus on quantitative mechanical characterization, manufacturable embodiments, and the integration of SPRDM-generated architectures into functional systems such as energy absorbers, deployable structures, and soft robotic components.

5. Conclusion

This work introduces the Spatial Poisson's Ratio Design Method (SPRDM) as a unified, geometry-driven framework for the systematic generation and classification of planar and spatial Poisson's ratio metamaterials. Building on the previously established planar base Z_2, we introduce a minimal spatial extension Z_3 and define a limited set of eight symmetry-based topological transformations that enable the reconstruction of known architectures and the generation of novel 1.5D, 2D, 2.5D, and 3D metamaterial families.

The SPRDM emphasizes topological generation rather than geometric optimization, providing a compact design space structured by dimensionality and chirality order. The introduction of a superchirality parameter allows planar and spatial chiral architectures to be treated consistently within a single framework. A concise naming protocol ensures traceability across the resulting families without overloading the main text.

Representative examples demonstrate how the SPRDM captures established auxetic, anepirretic, and chiral architectures, while also enabling new spatial configurations, including fully anepirretic and strain–twist metamaterials. To characterize structures beyond cubic symmetry, volume strain is proposed as a complementary, coordinate-independent descriptor, directly linked to bulk modulus and compressibility; detailed formulations and extended examples are provided in the Supplementary Information.

Overall, the SPRDM provides a generative and extensible methodology for architected materials design, suitable for guiding future numerical optimization, experimental realization, and application-driven exploration in mechanical metamaterials.

CRediT authorship contribution statement

Pierre Roberjot: Writing – review & editing, Writing – original draft, Methodology, Formal analysis, Conceptualization. **Rosalinde van den Bergh:** Formal analysis, Conceptualization. **Just L. Herder:** Validation, Supervision, Resources, Methodology.

Declaration of competing interest

The authors declare that they have no known competing financial interests or personal relationships that could have appeared to influence the work reported in this paper.

Acknowledgment

This publication is part of the project Mechanical Metamaterials for Compact Motion Systems (MECOMOS), project number 18940 of the Open Technology Program financed by the Dutch Research Council (NWO).

Appendix A. Supplementary data

Supplementary data to this article can be found online at https://doi.org/10.1016/j.matdes.2026.115796.

Data availability

No data was used for the research described in the article.

References

[1] H. Cho, D. Seo, and D.-N. Kim, "Mechanics of Auxetic Materials," in *Handbook of Mechanics of Materials*, S. Schmauder, C.-S. Chen, K. K. Chawla, N. Chawla, W. Chen, and Y. Kagawa, Eds., Singapore: Springer, 2019, pp. 733–757. Accessed: Mar. 31, 2023. [Online]. Available: doi:10.1007/978-981-10-6884-3_25.
[2] H.M.A. Kolken, A.A. Zadpoor, Auxetic mechanical metamaterials, RSC Adv. 7 (9) (2017) 5111–5129, https://doi.org/10.1039/C6RA27333E.
[3] J. Dagdelen, J. Montoya, M. de Jong, K. Persson, Computational prediction of new auxetic materials, Nat. Commun. 8 (1) (2017) 323, https://doi.org/10.1038/s41467-017-00399-6.
[4] A. Delissen, G. Radaelli, L.A. Shaw, J.B. Hopkins, J.L. Herder, Design of an isotropic metamaterial with constant stiffness and Zero Poisson's ratio over large deformations, J. Mech. Des. 140 (111405) (2018) Sep, https://doi.org/10.1115/1.4041170.
[5] A.B. Cairns, A.L. Goodwin, Negative linear compressibility, Phys. Chem. Chem. Phys. PCCP 17 (32) (Aug. 2015) 20449–20465, https://doi.org/10.1039/c5cp00442j.
[6] F. dell'Isola, et al., Advances in pantographic structures: design, manufacturing, models, experiments and image analyses, Contin. Mech. Thermodyn. 31 (4) (Jul. 2019) 1231–1282, https://doi.org/10.1007/s00161-019-00806-x.
[7] F.G. Broeren, V. van der Wijk, J.L. Herder, Spatial pseudo-rigid body model for the analysis of a tubular mechanical metamaterial, Math. Mech. Solids 25 (2) (Feb. 2020) 305–316, https://doi.org/10.1177/1081286519875500.
[8] Z. Meng, M. Liu, H. Yan, G. M. Genin, and C. Q. Chen, "Deployable mechanical metamaterials with multistep programmable transformation," *Sci. Adv.*, vol. 8, no. 23, p. eabn5460, Jun. 2022, doi: 10.1126/sciadv.abn5460.
[9] D. Rant, T. Rijavec, A. Pavko-Čuden, Auxetic textiles, Acta Chim. Slov. 60 (4) (2013) 715–723.
[10] H. Hu and A. Zulifqar, "Auxetic textile materials - A review," *J. Text. Eng. Fash. Technol.*, vol. Volume 1, no. Issue 1, Jan. 2017, doi: 10.15406/jteft.2017.01.00002.
[11] "Auxetic textile materials - A review," *J. Text. Eng. Fash. Technol.*, vol. Volume 1, no. Issue 1, Jan. 2017, doi: 10.15406/jteft.2017.01.00002.
[12] O. Duncan, et al., Review of auxetic materials for sports applications: expanding options in comfort and protection, Appl. Sci. 8 (6) (Jun. 2018) 941, https://doi.org/10.3390/app8060941.
[13] R. Lakes, Foam structures with a negative Poisson's ratio, Science 235 (4792) (Feb. 1987) 1038–1040, https://doi.org/10.1126/science.235.4792.1038.
[14] J.N. Grima, L. Mizzi, K.M. Azzopardi, R. Gatt, Auxetic perforated mechanical metamaterials with randomly oriented cuts, Adv. Mater. 28 (2) (2016) 385–389, https://doi.org/10.1002/adma.201503653.
[15] K. Bertoldi, V. Vitelli, J. Christensen, and M. van Hecke, "Flexible mechanical metamaterials," *Nat. Rev. Mater.*, vol. 2, no. 11, Art. no. 11, Oct. 2017, doi: 10.1038/natrevmats.2017.66.
[16] A. Hasse, K. Mauser, Poisson induced bending actuator for soft robotic systems, Soft Robot. 7 (2) (Apr. 2020) 155–167, https://doi.org/10.1089/soro.2018.0163.
[17] M. Balan P, J. Mertens A, and M. V. A. R. Bahubalendruni, "Auxetic mechanical metamaterials and their futuristic developments: A state-of-art review," *Mater. Today Commun.*, vol. 34, p. 105285, Mar. 2023, doi: 10.1016/j.mtcomm.2022.105285.
[18] U.D. Larsen, O. Signund, S. Bouwsta, Design and fabrication of compliant micromechanisms and structures with negative Poisson's ratio, J. Microelectromechanical Syst. 6 (2) (Jun. 1997) 99–106, https://doi.org/10.1109/84.585787.
[19] K. Wojciechowski, Poisson's ratio of anisotropic systems, CMST 11 (1) (2005) 73–79, https://doi.org/10.12921/cmst.2005.11.01.73-79.
[20] J.N. Grima, D. Attard, R. Gatt, Truss-type systems exhibiting negative compressibility, Phys. Status Solidi B 245 (11) (2008) 2405–2414, https://doi.org/10.1002/pssb.200880267.
[21] T. Meier, et al., Obtaining auxetic and isotropic metamaterials in counterintuitive design spaces: an automated optimization approach and experimental characterization, npj Comput. Mater. 10 (1) (Jan. 2024) 3, https://doi.org/10.1038/s41524-023-01186-2.
[22] A. Rafsanjani, D. Pasini, Bistable auxetic mechanical metamaterials inspired by ancient geometric motifs, Extreme Mech. Lett. 9 (Dec. 2016) 291–296, https://doi.org/10.1016/j.eml.2016.09.001.
[23] C. Zhang, F. Lu, T. Wei, H. Wang, F. Liu, Y. Zhu, Windmill-shaped metamaterials achieving negative thermal expansion, Eng. Struct. 336 (Aug. 2025) 120488, https://doi.org/10.1016/j.engstruct.2025.120488.

[24] Y. Zhu, X. Wu, X. Rui, D. Gan, Q. Wang, C. Zhang, On the design and in-plane crashworthiness of a novel extendable assembled auxetic honeycomb, Thin-Walled Struct. 211 (Jun. 2025) 113123, https://doi.org/10.1016/j.tws.2025.113123.
[25] I. Fernandez-Corbaton, et al., New twists of 3D chiral metamaterials, Adv. Mater. 31 (26) (2019) 1807742, https://doi.org/10.1002/adma.201807742.
[26] K.K. Dudek, A. Drzewiński, M. Kadic, Self-rotating 3D chiral mechanical metamaterials, Proc. R. Soc. Math. Phys. Eng. Sci. 477 (2251) (Jul. 2021) 20200825, https://doi.org/10.1098/rspa.2020.0825.
[27] P. Roberjot, J.L. Herder, A unified design method for 2D auxetic metamaterials based on a minimal auxetic structure, Int. J. Solids Struct. 295 (Jun. 2024) 112777, https://doi.org/10.1016/j.ijsolstr.2024.112777.
[28] P. Roberjot, J.L. Herder, A unified planar Poisson's ratio design method (PPRDM) for meiotic metamaterials that exhibit negative compressibility based on a minimal chiral meiotic structure, Int. J. Solids Struct. 320 (Sep. 2025) 113494, https://doi.org/10.1016/j.ijsolstr.2025.113494.
[29] S. Duan, L. Xi, W. Wen, D. Fang, A novel design method for 3D positive and negative Poisson's ratio material based on tension-twist coupling effects, Compos. Struct. 236 (Mar. 2020) 111899, https://doi.org/10.1016/j.compstruct.2020.111899.
[30] C.Q. Lai, K. Markandan, Z. Lu, Anomalous elastic response of a 3D anti - tetrachiral metamaterial, Int. J. Mech. Sci. 192 (Feb. 2021) 106142, https://doi.org/10.1016/j.ijmecsci.2020.106142.
[31] J.H. Park, et al., 3D printing of Poly-ε-caprolactone (PCL) Auxetic implants with advanced performance for large volume soft tissue engineering, Adv. Funct. Mater. 33 (24) (2023) 2215220, https://doi.org/10.1002/adfm.202215220.
[32] J.T.B. Overvelde, J.C. Weaver, C. Hoberman, K. Bertoldi, Rational design of reconfigurable prismatic architected materials, Nature 541 (7637) (Jan. 2017) 347–352, https://doi.org/10.1038/nature20824.
[33] A. Sorrentino and D. Castagnetti, "Geometrically tunable architected materials designed from prismatic rotating units," *Proc. Inst. Mech. Eng. Part J. Mater. Des. Appl.*, vol. 238, no. 9, pp. 1690–1704, Sep. 2024, doi: 10.1177/14644207241229995.
[34] C. Luo, C.Z. Han, X.Y. Zhang, X.G. Zhang, X. Ren, Y.M. Xie, Design, manufacturing and applications of auxetic tubular structures: a review, Thin-Walled Struct. 163 (Jun. 2021) 107682, https://doi.org/10.1016/j.tws.2021.107682.
[35] L. D'Alessandro, V. Zega, R. Ardito, A. Corigliano, 3D auxetic single material periodic structure with ultra-wide tunable bandgap, Sci. Rep. 8 (1) (Feb. 2018) 2262, https://doi.org/10.1038/s41598-018-19963-1.
[36] F. Wang, Systematic design of 3D auxetic lattice materials with programmable Poisson's ratio for finite strains, J. Mech. Phys. Solids 114 (May 2018) 303–318, https://doi.org/10.1016/j.jmps.2018.01.013.
[37] A.R. Hadjesfandiari, G.F. Dargush, Couple stress theory for solids, Int. J. Solids Struct. 48 (18) (Sep. 2011) 2496–2510, https://doi.org/10.1016/j.ijsolstr.2011.05.002.
[38] B. Lemkalli, K. Muamer, Y. Badri, S. Guenneau, B. Abdenbi, and Y. Achaoui, *Mapping of Elastic Properties of Twisting Metamaterials onto Micropolar Continuum using Static Calculations*. 2022.
[39] Z. Wei, Y. Wu, H. Lai, and J. Qian, "Compression-Twist Coupling Mechanical Metamaterials with Programmed Bistability," *Acta Mech. Solida Sin.*, pp. 1–9, Feb. 2025, doi: 10.1007/s10338-025-00583-y.
[40] M.A. Fortes, M. Teresa Nogueira, The poison effect in cork, Mater. Sci. Eng. A 122 (2) (1989) 227–232, https://doi.org/10.1016/0921-5093(89)90634-5.
[41] R. Li, Y. Yao, X. Kong, A class of reconfigurable deployable platonic mechanisms, Mech. Mach. Theory 105 (Nov. 2016) 409–427, https://doi.org/10.1016/j.mechmachtheory.2016.07.019.
[42] R. Li, H. Chen, J.H. Choi, Topological assembly of a deployable Hoberman flight ring from DNA, Small 17 (11) (2021) 2007069, https://doi.org/10.1002/smll.202007069.
[43] Y. Zhang, Z. Qian, H. Huang, X. Yang, and B. Li, "A Snake-Inspired Swallowing Robot Based on Hoberman's Linkages," *J. Mech. Robot.*, vol. 14, no. 060905, Apr. 2022, doi: 10.1115/1.4054308.
[44] M.R. Sloan, J.R. Wright, K.E. Evans, The helical auxetic yarn – a novel structure for composites and textiles; geometry, manufacture and mechanical properties, Mech. Mater. 43 (9) (Sep. 2011) 476–486, https://doi.org/10.1016/j.mechmat.2011.05.003.
[45] T.J. Cuthbert, B.C. Hannigan, P. Roberjot, A.V. Shokurov, C. Menon, HACS: helical auxetic yarn capacitive strain sensors with sensitivity beyond the theoretical limit, Adv. Mater. 35 (10) (2023) 2209321, https://doi.org/10.1002/adma.202209321.
[46] B. C. Hannigan, T. J. Cuthbert, C. Ahmadizadeh, and C. Menon, "Distributed sensing along fibers for smart clothing," *Sci. Adv.*, vol. 10, no. 12, p. eadj9708, Mar. 2024, doi: 10.1126/sciadv.adj9708.
[47] R. Gatt, et al., Hierarchical auxetic mechanical metamaterials, Sci. Rep. 5 (1) (Feb. 2015) 8395, https://doi.org/10.1038/srep08395.
[48] M. Morvaridi, et al., Hierarchical auxetic and isotropic porous medium with extremely negative Poisson's ratio, Extreme Mech. Lett. 48 (Oct. 2021) 101405, https://doi.org/10.1016/j.eml.2021.101405.
[49] Y. Liu, D.-W. Shu, H. Lu, D. Lau, Y.-Q. Fu, 3D printable spatial fractal structures undergoing auxetic elasticity, Extreme Mech. Lett. 66 (Jan. 2024) 102112, https://doi.org/10.1016/j.eml.2023.102112.
[50] Y. Zhu, Z. Chen, Y. Zhu, M. Gresil, Y. Tang, Bio-inspired perturbated hierarchical mechanical metamaterial for energy absorption, Int. J. Mech. Sci. 307 (Dec. 2025) 110847, https://doi.org/10.1016/j.ijmecsci.2025.110847.
[51] P. Surówka, A. Souslov, F. Jülicher, D. Banerjee, Odd Cosserat elasticity in active materials, Phys. Rev. E 108 (6) (Dec. 2023) 064609, https://doi.org/10.1103/PhysRevE.108.064609.
[52] M.A. Bessa, P. Glowacki, M. Houlder, Bayesian machine learning in metamaterial design: fragile becomes supercompressible, Adv. Mater. 31 (48) (2019) 1904845, https://doi.org/10.1002/adma.201904845.
[53] M. Houlder and M. Bessa, "Design of a Super-Compressible Metamaterial: An Experimental Investigation Guided by Machine Learning," *Masters Thesis*, 2019, Accessed: Feb. 22, 2023. [Online]. Available: http://resolver.tudelft.nl/uuid:3716e88c-ea9a-413d-a310-af6cad5009c3.
[54] R.H. Baughman, S. Stafström, C. Cui, S.O. Dantas, Materials with negative compressibilities in one or more dimensions, Science 279 (5356) (Mar. 1998) 1522–1524, https://doi.org/10.1126/science.279.5356.1522.
[55] Y. Gao, X. Wei, X. Han, Z. Zhou, J. Xiong, Novel 3D auxetic lattice structures developed based on the rotating rigid mechanism, Int. J. Solids Struct. 233 (Dec. 2021) 111232, https://doi.org/10.1016/j.ijsolstr.2021.111232.